Advances in Automobile Engineering
ISSN: 2167-7670

Trivedi et al., Adv Automob Eng 2015, 4:1
DOI; 10.4172/2167-7670.1000119

Research Article Open Access

Evaluation of Biofield Treatment on Physical and Structural Properties of Bronze Powder

Trivedi MK[2], Nayak G[2], Patil S[2], Tallapragada RM[2], Latiyal O[1] and Jana S[1]*

[1]*Trivedi Science Research Laboratory Pvt. Ltd., Bhopal, Madhya Pradesh, India*
[2]*Trivedi Global Inc., 10624 S Eastern Avenue Suite A-969, Henderson, NV 89052, USA*

Abstract

Bronze, a copper-tin alloy, widely utilizing in manufacturing of gears, bearing, and packing technologies due to its versatile physical, mechanical, and chemical properties. The aim of the present work was to evaluate the effect of biofield treatment on physical and structural properties of bronze powder. Bronze powder was divided into two samples, one served as control and the other sample was received biofield treatment. Control and treated bronze samples were characterized using x-ray diffraction (XRD), particle size analyzer, scanning electron microscopy (SEM), and Fourier transform infrared (FT-IR) spectroscopy. XRD result showed that the unit cell volume was reduced upto 0.78% on day 78 in treated bronze as compared to control. Further, the crystallite size was significantly reduced upto 49.96% in treated bronze sample on day 106 as compared to control. In addition, the biofield treatment has significantly reduced the average particle size upto 18.22% in treated bronze powder as compared to control. SEM data showed agglomerated and welded particles in control bronze powder, whereas fractured morphology at satellites boundaries were observed in treated bronze. The yield strength of bronze powder calculated using Hall-Petch equation, was significantly changed after biofield treatment. The FT-IR analysis showed that there were three new peaks at 464 cm^{-1}, 736 cm^{-1}, and 835 cm^{-1} observed in treated bronze as compared to control; indicated that the biofield treatment may alter the bond properties in bronze. Therefore, the biofield treatment has substantially altered the characteristics of bronze at physical and structural level.

Keywords: Biofield treatment; Bronze; X-ray diffraction; FT-IR; Particle size; SEM

Introduction

Bronze is a metallic alloy, primarily consist of copper and tin in 90:10 ratio, which is also known as "true bronze". Some other elements such as arsenic, phosphorus, aluminium, manganese, and silicon are also blended in bronze to enhance its mechanical properties [1,2]. The variation in elemental composition in bronze significantly affects its mechanical and chemical characteristics [3]. Furthermore, the bronze, primarily exist in FCC (face centred cubic) crystal structure, and the different size of the tin atoms as compared to copper substantially changes this structure, which confers excellent properties. Sidot et al. reported that lattice parameter of FCC bronze unit cell increases with increase in tin content and vice versa [4]. Moreover, the influences of crystallite size on the mechanical properties of metals and alloys have been known for many years. Two scientist Hall and Petch proposed the formula, which demonstrated the inverse relation between yield strength and crystallite size [5]. Nevertheless, bronze is widely utilized in the production of bearing, operating under heavy loads at high speeds. These bearing are used in many rotating parts such as fans, jet engines, automobile parts, industrial equipment, and appliances etc. Beside this, it is also used in filters and decorative paints. Bronze powder is mainly produced via electrolysis process, vapour deposition, and high-energy ball mill method [6]. Further, it is reported that the mechanical properties in bronze can be modulated through various kind of sintering processes [7,8]. In these sintering processes, high temperature and costly equipment setup are required to achieve the desired mechanical properties. After considering of alloy properties and cost aspect, authors wanted to investigate an alternative and economically safe approach that could be beneficial in global application to modify the structural and mechanical properties of bronze powder.

A physicist, William Tiller proposed the existence of a new force related to human body, in addition to four well known fundamental forces of physics: gravitational force, strong force, weak force, and electromagnetic force. Fritz-Albert, a German biophysicist proposed that human physiology shows a high degree of order and stability due to their coherent dynamic states [9-12]. Furthermore, a human has ability to harness the energy from environment/universe and can transmit into any object (living or non-living) around the globe. The objects always receive the energy and responded into useful way and that is called biofield energy. This process is known as biofield treatment. Mahendra Trivedi's biofield treatment has been applied to transform the structural, physical, and chemical properties of various metals and ceramics [13-20]. In material science, this biofield treatment has substantially changed the particle size, surface area and lattice parameters in various ceramic powders such as vanadium pentoxide (V_2O_5), zirconium oxide (ZrO_2), and silicon dioxide (SiO_2) [18,19]. The biofield treatment has also transformed the characteristics in several other fields like biotechnology [21,22], microbiology [23-25], and in agricultural science [26-28].

Based on the outstanding results achieved by biofield treatment on different materials and considering the industrial significance of bronze powder, the present study was undertaken to evaluate the impact of biofield treatment on physical and structural properties of bronze powder.

***Corresponding author:** Dr. Snehasis Jana, Trivedi Science Research Laboratory Pvt. Ltd., Hall-A, Chinar Mega Mall, Chinar Fortune City, Hoshangabad Road, Bhopal- 462026 Madhya Pradesh, India, Tel: +91-755-6660006; E-mail: publication@trivedisrl.com

Received June 22, 2015; **Accepted** July 03, 2015; **Published** July 07, 2015

Citation: Trivedi MK, Nayak G, Patil S, Tallapragada RM, Latiyal O, et al. (2015) Evaluation of Biofield Treatment on Physical and Structural Properties of Bronze Powder. Adv Automob Eng 4: 119. doi:10.4172/2167-7670.1000119

Experimental

Bronze powder was procured from Alfa Aesar, USA. The bronze powder sample was divided into two parts, one part was considered as control and another part was subjected to Mr. Trivedi's biofield treatment, referred as treated. The control and treated samples were characterized using x-ray diffraction (XRD), particle size analyzer, scanning electron microscopy (SEM), and Fourier transform infrared (FT-IR) spectroscopy.

X-ray diffraction study

XRD analysis was carried out on Phillips, Holland PW 1710 X-ray diffractometer system, which had a copper anode with nickel filter. The radiation of wavelength used by the XRD system was 1.54056 Å. The data obtained from this XRD were in the form of a chart of 2θ vs. intensity and a detailed table containing peak intensity counts, d value (Å), peak width (θ^0), relative intensity (%) etc. Additionally, PowderX software was used to calculate lattice parameter and unit cell volume.

The crystallite size (G) was calculated by using formula:

$$G = k\lambda / (bCos\theta),$$

Here, λ is the wavelength of radiation used and k is the equipment constant (=0.94). However, the percentage change in all parameters such as lattice parameter, unit cell volume and crystallite size was calculated using the following equation:

$$\text{Percent change in lattice parameter} = \left[(a_t - a_c)/a_c\right] \times 100$$

Where, a_c and a_t are lattice parameter value of control and treated powder samples respectively

$$\text{Percent change in unit cell volume} = \left[(V_t - V_c)/V_c\right] \times 100$$

Where, V_c and V_t are the unit cell volume of control and treated powder samples respectively

$$\text{Percent change in crystallite size} = \left[(G_t - G_c)/G_c\right] \times 10$$

Where, G_c and G_t are crystallite size of control and treated powder samples respectively. The XRD analysis was carried out on day 1, 10, 78, 106 and 117 day referred as control, T1, T2, T3, and T4 respectively.

Particle size analysis

For particle size analysis, laser particle size analyzer SYMPATEC HELOS-BF was used, which had a detection range of 0·1-875 µm. The particle size data was collected in the form of a chart of particle size vs. cumulative percentage. Three parameters of particle sizes viz. d_{50}, d_{90}, and d_{99} (size below which 50%, 90%, and 99% particles are present, respectively) were calculated from the particle size distribution curve. The percent change in particle sizes were calculated using following equation:

$$\%\,\text{change in particle size}, d_{50} = \frac{[(d_{50})_{\text{Treated}} - [(d_{50})_{\text{Control}}]}{(d_{50})_{\text{Control}}} \times 100$$

Where, $(d_{50})_{\text{Control}}$ and $(d_{50})_{\text{Treated}}$ are the particle size, d_{50} of control and treated samples respectively. Similarly, the percent change in particle size d_{90} and d_{99} were calculated. The particle size were evaluated on day 1, 12, 91, 97 and 115 for control, T1, T2, T3, and T4 respectively.

Scanning electron microscopy (SEM)

In order to study the changes in surface morphology of bronze powder after biofield treatment, the control and treated sample were analyzed on day 20 using SEM, the JEOL JSM-6360 instrument.

FT-IR spectroscopy

To study the impact of biofield treatment at atomic bonding level in bronze powder, the FT-IR analysis was done on Shimadzu, Fourier transform infrared (FT-IR) spectrometer with frequency range of 300-4000 cm^{-1}. FT-IR analysis was carried out on day 1, day 71 and day 82 for control, T1, and T2, respectively.

Results and Discussion

X-ray diffraction study

The XRD results are presented in Table 1. It was observed that the lattice parameter of the unit cell reduced by 0.2%, 0.26%, 0.19%, and 0.07% in treated bronze T1, T2, T3, and T4 respectively, as compared to control. The percent change in lattice parameter is also known as lattice strain. Further, the decreased lattice parameter led to reduce the volume of unit cell by 0.61%, 0.78%, 0.56%, and 0.21% in treated samples T1, T2, T3, and T4 respectively as compared to control (Figure 1). The percent change in lattice parameter and unit cell volume was found maximum on day 78 (T2). In general, when the applied stress is compressive the change in strain is negative while a positive value indicates a tensile stress. Thus, negative strain in all treated bronze sample indicated that a compressive stress was probably acted on treated bronze sample after biofield treatment. It is possible that biofield treatment could be transferred the energy to bronze powder and that may induced milling in the powder. Hence, this high energy milling may lead to persuade the compressive stress and changed the lattice parameter [16-19]. Moreover, the crystallite size was 88.96 nm in control sample, however it was changed to 148.96 nm, 111.30 nm, 44.52 nm, and 148.38 nm in treated samples on day 10 (T1), day 78 (T2), day 106 (T3), and day 117 (T4) respectively. The percent change in crystallite size is presented in Figure 2, it showed that the crystallite size was increased upto 66.79% on day 10, then started to decrease upto 49.96% on day 106 (T3) as compared to control. It is possible that the tin (Sn) atoms might be diffused into copper (Cu) due to biofield energy that may lead to coalescence of grains and increase the crystallite size [7]. Furthermore, the existence of severe lattice strains is evidenced by the change in lattice parameters (Figure 1). The presence of this internal strain may lead to fracture the grains into sub grains and decrease the crystallite size upto day 106 [19]. Moreover, the relation between strength of material and crystallite size is given by Hall-Patch equation as given below:

$$\sigma = \sigma_\circ + k/\sqrt{G} \quad (1)$$

Where, σ is strength of the material $\sigma_\circ$, is a material constant for the starting stress for dislocation movement, k is the strengthening coefficient, G is crystallite size.

Dybiec et al. reported the material constant, σ_o =58.9 MPa and k=0.3689 MPa $m^{1/2}$ for bronze [29]. These parameters were used to calculate the yield strength of control and treated bronze powder. The yield strength of all samples were calculated using equation (1) and

Group	Lattice Parameter (Å)	Unit Cell Volume (×$10^{-23}$$cm^3$)	Crystallite size (nm)
Control	3.6224	4.753	88.96
Treated T1	3.6151	4.724	148.38
Treated T2	3.6129	4.716	111.30
Treated T3	3.6156	4.727	44.52
Treated T4	3.6199	4.743	148.36

Table 1: X-ray diffraction analysis of bronze powder.

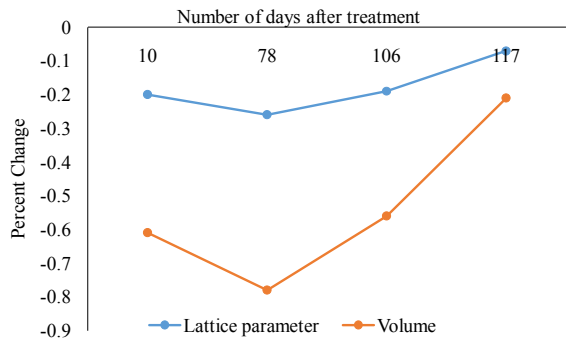

Figure 1: Percent change in lattice parameter and unit cell volume in biofield treated bronze as compared to control.

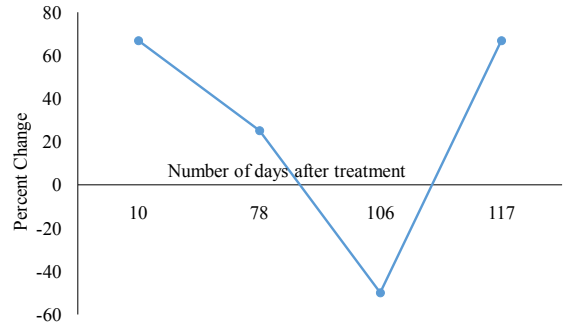

Figure 2: Percent change in crystallite size in biofield treated bronze as compared to control.

percent change in treated bronze powder as compared to control. It was observed that the yield strength was reduced by 9% on day 10 (T1) and then increased upto 16.50% on day 106 (T3), as compared to control, after biofield treatment. Nevertheless, the yield strength was again decreased by 8.99% on day 117 as compared to control. Overall, the graph indicates that bronze showed the higher yield strength in time period of day 82 to day 115 (Figure 3). This variation in yield strength in treated bronze powder could be due to change of crystallite size after biofield treatment as explained by Hall and Petch. The strength of materials can be modulated by changing the crystallite size and this could be due to interactions of dislocations with crystallite boundaries as they move. In this phenomenon, the crystallites boundaries hindered the movement of dislocation gliding along the slip planes and increased the yield strength [30]. It is also reported that the reduction in crystallite size leads to increase the grain boundaries and vice versa. Thus, it is hypothesized that the change in crystallite size after biofield treatment in bronze could alter the yield strength.

Particle size analysis

In order to understand the effect of biofield treatment on particle size, several range i.e. d_{50}, $d_{90,}$ andd_{99} were calculated and results are presented in Table 2 and Figure 4. It was observed that the particle sizes of d_{50}, $d_{90,}$ andd_{99} were increased by 5.15, 8.21, 12.17% respectively, as compared to control on day 12. It may be due to agglomeration of finer particles through high energy milling that probably induced by biofield treatment. Furthermore, the d_{50}, $d_{90,}$ and d_{99} were reduced by 16.24, 18.71, 18.75% respectively, as compared to control on day 91. This can be possible if coarser particles get fracture to smaller particle size. Further, on day 97 the particle size of d_{50}, $d_{90,}$ and d_{99} were reduced by 18.22, 12.89, and 11.95% respectively as compared to control. In addition, particle sizes of d_{50}, $d_{90,}$ and d_{99} were also reduced by 13.47, 8.78, and 9.96% respectively on day 115, as compared to control. Overall, the graph showed that particle of each size i.e. finer to coarser, were reduced as increase in number of days after biofield treatment (Figure 4). It is well known that the bronze powder particles are polycrystalline i.e. it consist of many grains. In polycrystalline particles,

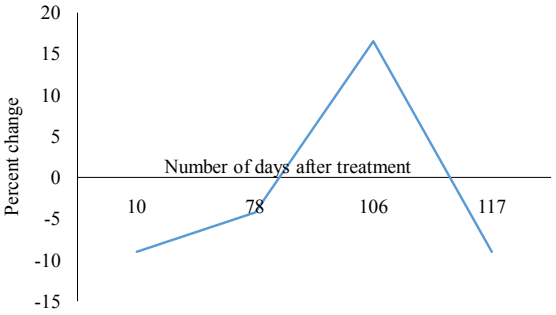

Figure 3: Percent change in yield strength of biofield treated bronze as compared to control.

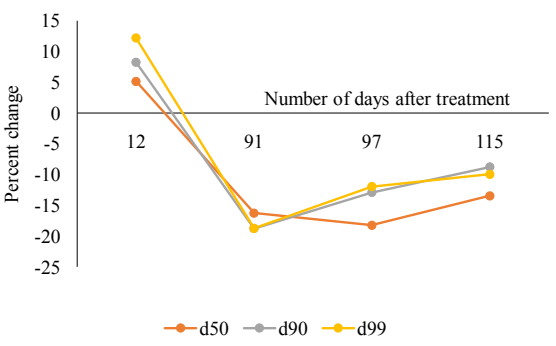

Figure 4: Percent change in particle size in biofield treated bronze as compared to control.

Groups	d_{50} (µm)	d_{90} (µm)	d_{99} (µm)
Control	50.50	94.26	135.60
Treated T1	53.10	102.00	152.10
Treated T2	42.30	76.59	110.20
Treated T3	41.30	82.11	119.40
Treated T4	43.70	85.98	122.10

d_{50}, d_{90}, and d_{99}, size below which 50%, 90%, and 99% particles are present, respectively

Table 2: Particle size analysis of bronze powder.

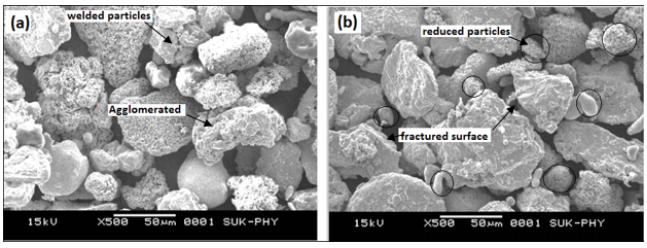

Figure 5: The SEM images of (a) control and (b) treated bronze powder.

crystallite boundaries are the structural weak points [16,17]. Hence, it is hypothesized that these weak boundaries may fracture under stress and reduced particle size.

SEM analysis

The SEM images of control and treated bronze samples at magnification of 500x are shown in Figure 5. The diffusion welded and agglomerated particles were observed in control bronze with size range of 1-100 µm. However, in treated bronze powder, fractured surface morphology along with satellites and intra-particle boundaries were observed. Furthermore, the treated bronze particles were in the size range of 1-75 µm. It indicates that the coarser particles may fracture into finer after biofield treatment that possibly reduces the particle size [17]. Furthermore, in order to study the bronze powder at atomic bonding level, samples were analyzed using FT-IR.

FT-IR spectroscopy

FT-IR spectrum of control and treated bronze samples are shown in Figures 6-8. In all these spectra, absorption bands in region of range 4000-300 cm^{-1} were observed. The FT-IR spectra showed an absorption peak at wavenumber 1541 cm^{-1} (Control and T1) and 1550 cm^{-1} (T2), which characterized the O-H bending. However, the bands at wavenumber 3734 cm^{-1} (control and T1) and 3749 cm^{-1} (T2) were assigned to O-H stretching vibration that may be due to moisture absorption by samples [31,32]. Furthermore, the peak at 648 cm^{-1}(control) and 650 cm^{-1} (T1), and 663 cm^{-1} (T2) can be attributed to Sn-O stretching vibrations [32]. This indicates that wavenumber shifted toward higher side, after biofield treatment, which could be due to alteration in Sn-O bond strength. Besides this, the IR spectra of treated (T2) showed three new peaks at wavenumber 464 cm^{-1}, 736 cm^{-1}, and 835 cm^{-1} (Figure 8). The peaks at 736 cm^{-1}, and 835 cm^{-1} can be attributed to Cu-O-H bending mode, whereas the emergence of peak at 464 cm^{-1} could be due to Cu-O vibrations [33,34]. Thus, it is presumed that biofield treatment may be acting at atomic bonding level to cause these modifications.

Conclusion

In summary, the biofield treatment has significantly altered the lattice strain, crystallite size, particle size and surface morphology in

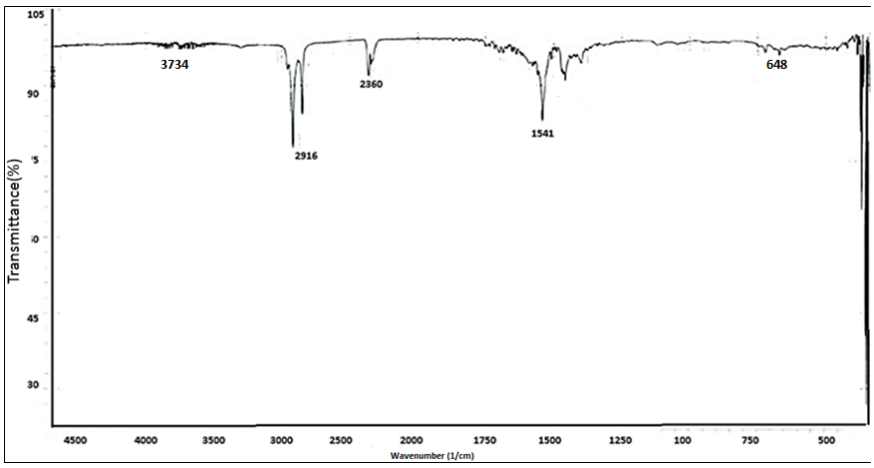

Figure 6: FT-IR spectrum of control bronze powder.

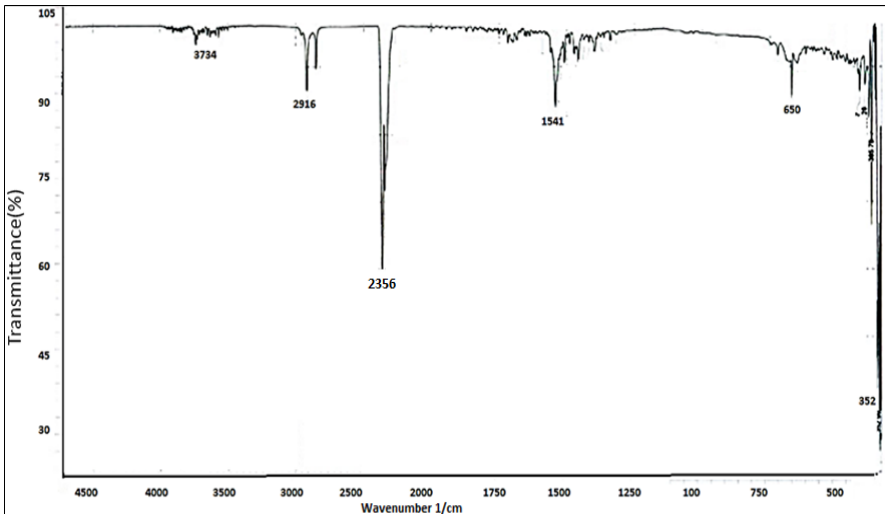

Figure 7: FT-IR spectrum of biofield treated bronze powder (T1).

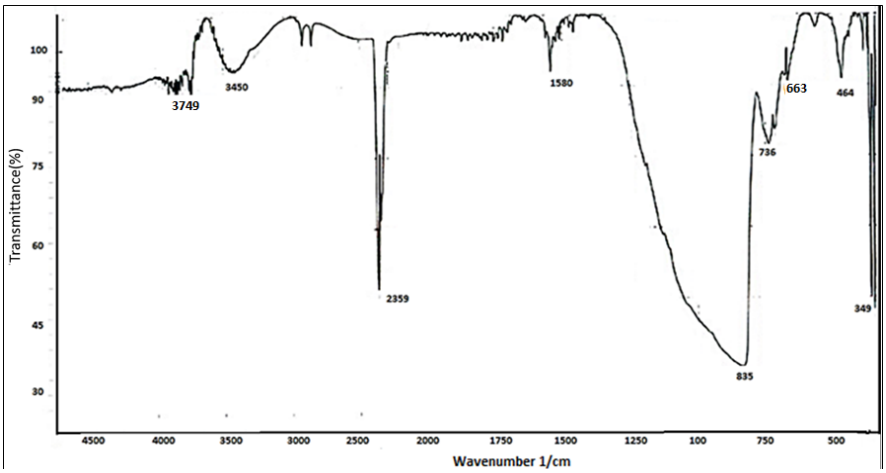

Figure 8: FT-IR spectrum of biofield treated bronze powder (T2).

bronze powder as compared to control. XRD data revealed that the unit cell volume was reduced upto 0.78% as compared to control. This could be due to compressive stress generated during high energy milling through biofield treatment. Besides this, the reduction in crystallite size upto 49.9% may lead to increase the mechanical strength of the bronze powder after biofield treatment. In addition, biofield treatment has significantly reduced the particle size upto 18.22% in bronze powder as compared to control. SEM data showed fractured surfaces in treated sample whereas welded particles were observed in control sample. Furthermore, the FT-IR analysis data suggest that there were three new peaks at 464 cm^{-1}, 736 cm^{-1}, and 835 cm^{-1} found in treated bronze as compared to control; indicated that there might be an alteration of bond properties in bronze after biofield treatment. Overall, the biofield treatment has substantially altered the characteristics of bronze at physical and structural level. Thus, it is postulated that the biofield treated bronze powder could be more useful in bearing and gear applications in automobiles.

Acknowledgement

We thank Dr. Cheng Dong of NLSC, Institute of Physics, and Chinese academy of Sciences for supporting in using PowderX software for analyzing X-ray Diffraction data.

References

1. Weaver ME (1997) Conserving buildings: A manual of techniques and materials. J Wiley and Sons, New York.
2. Gayle M (1992) Metals in America's historic buildings. Part I. A historical survey of metals. Washington, DC, National Park Service.
3. Zohner LW (1995) Architectural Metals. J Wiley and Sons, New York.
4. Sidot E, Kahn HA, Cesari E, Robbiola L (2005) The lattice parameter of bronzes as a function of solute content: Application to archaeological materials. Mater Sci Eng A 393: 147-156.
5. Gryziecki J (1977) Metallurgy and foundry practice. Bulletin 78, University of Mining and Metallurgy, Krakow.
6. Nasonova MN, Galinker VS, Gorbatyuk VA, Klimuk LL (1976) Production of bronze powders from tripolyphosphate electrolytes. Sov Powder Metall Met Ceram 15: 83-85.
7. Agarwal N, Sethi G, Upadhyaya A, Agarawal D, Roy R, et al. (2003) Microstructural and microhardness studies of microwave sintered Cu-12Sn bronze alloys. Trans PMAI 29: 61-65.
8. Bashir F, Butt MZ, Saleemi F (2008) Microstructural and hardness studies of Cu-10 wt percent Sn alloy under different aging conditions. J Mater Eng Perform 17: 123-126.
9. Popp FA, Chang JJ, Herzog A, Yan Z, Yan Y, et al. (2002) Evidence of non-classical (squeezed) light in biological systems. Phys Lett 293: 98-102.
10. Popp FA, Gu Q, Li KH (1994) Biophoton emission: Experimental background and theoretical approaches. Mod Phys Lett B 8: 21-22.
11. Popp FA (1992) Recent advances in biophoton research and its applications. World Scientific Publishing Co Pte Ltd.
12. Cohen S, Popp FA (2003) Biophoton emission of the human body. Indian J Exp Biol 41: 440-445.
13. Trivedi MK, Tallapragada RM (2008) A transcendental to changing metal powder characteristics. Met Powder Rep 63: 22-28.
14. Trivedi MK, Tallapragada RM (2009) Effect of super consciousness external energy on atomic, crystalline and powder characteristics of carbon allotrope powders. Mater Res Innov 13: 473-480.
15. Dhabade VV, Tallapragada RM, Trivedi MK (2009) Effect of external energy on atomic, crystalline and powder characteristics of antimony and bismuth powders. Bull Mater Sci 32: 471-479.
16. Trivedi MK, Patil S, Tallapragada RM (2012) Thought intervention through bio field changing metal powder characteristics experiments on powder characteristics at a PM plant. Proceeding of the 2nd International conference on Future control and automation 2: 247-252.
17. Trivedi MK, Patil S, Tallapragada RM (2013) Effect of biofield treatment on the physical and thermal characteristics of silicon, tin and lead powders. J Material SciEng 2: 125.
18. Trivedi MK, Patil S, Tallapragada RM (2013) Effect of biofield treatment on the physical and thermal characteristics of vanadium pentoxide powder. J Material SciEng S11: 001.
19. Trivedi MK, Patil S, Tallapragada RM (2014) Atomic, crystalline and powder characteristics of treated zirconia and silica powders. J Material Sci Eng 3: 144.
20. Trivedi MK, Patil S, Tallapragada RM (2015) Effect of biofield treatment on the physical and thermal characteristics of aluminium powders. IndEng Manage 4: 151.
21. Patil S, Nayak GB, Barve SS, Tembe RP, Khan RR (2012) Impact of biofield treatment on growth and anatomical characteristics of Pogostemoncablin (Benth.). Biotechnology 11: 154-162.
22. Altekar N, Nayak G (2015) Effect of biofield treatment on plant growth and adaptation. J Environ Health Sci 1: 1-9.
23. Trivedi MK, Patil S, Bhardwaj Y (2008) Impact of an external energy on Staphylococcus epidermis in relation to antibiotic susceptibility and biochemical reactions-An experimental study. J Accord Integr Med 4: 230-235.
24. Trivedi MK, Patil S (2008) Impact of an external energy on Yersinia

enterocolitica in relation to antibiotic susceptibility and biochemical reactions: An experimental study. Internet J Alternat Med 6.

25. Trivedi MK, Patil S, Bhardwaj Y (2009) Impact of an external energy on *Enterococcus* in relation to antibiotic susceptibility and biochemical reactions-An experimental study. J Accord Integr Med 5: 119-130.
26. Shinde V, Sances F, Patil S, Spence A (2012) Impact of biofield treatment on growth and yield of lettuce and tomato. Aust J Basic Appl Sci 6: 100-105.
27. Lenssen AW (2013) Biofield and fungicide seed treatment influences on soybean productivity, seed quality and weed community. Agric J 8: 138-143.
28. Sances F, Flora E, Patil S, Spence A, Shinde V (2013) Impact of biofield treatment on ginseng and organic blueberry yield. AGRIVITA J Agric Sci 35.
29. Dybiec H (1990) TheHall-Petchrelation in Cu-6wt percent Sn bronze. J Mater Sci Lett 9: 678-680.
30. Callister WD (2008) Fundamentals of materials science and engineering: An integrated approach. (3rdedn), John Wiley and Sons.
31. Niasari MS, Davar F, Mir N (2008) Synthesis and characterization of metallic copper nanoparticles via thermal decomposition. Polyhedron 27: 3514-3518.
32. Petrov T, Markova-Deneva I, Chauvet O, Nikolov R, Denev I (2012) SEM and FT-IR spectroscopy study of Cu, Sn and Cu-Sn nanoparticles. J University ChemTechnol Metall 47: 197-206.
33. Zhang X, Wallinder IO, Leygraf C (2014) Mechanistic studies of corrosion product flaking on copper and copper-based alloys in marine environments. Corr Sci 85: 15-25.
34. Coates J (2000) Interpretation of infrared spectra, a practical approach. John Wiley and Sons Ltd., Chichester.